



Mapping object space dimensions: New insights from temporal dynamics

Alexis Kidder^a, Genevieve L. Quek^b, Tijl Grootswagers^{b,c}

^aDepartment of Psychological and Brain Sciences, Dartmouth College, Hanover, NH, United States

^bThe MARCS Institute for Brain, Behaviour and Development, Western Sydney University, Sydney, NSW Australia

^cSchool of Computer, Data, and Mathematical Sciences, Western Sydney University, Sydney, NSW Australia

Corresponding Author: Alexis Kidder (alexis.kidder.gr@dartmouth.edu)

ABSTRACT

How is object information organized in high-level visual cortex? A recent comprehensive model of object space in macaques defines object space via orthogonal axes of animacy and aspect ratio (i.e., stubby vs. spiky) (Bao et al., 2020). However, when using object stimuli that dissociated category, animacy, and aspect ratio in human fMRI, object space appeared to be principally defined by category and animacy, with limited tuning of aspect ratio in object-selective regions (Yargholi & Op de Beeck, 2023). Here, we aimed to further clarify the contribution of aspect ratio during object processing by using whole-brain electroencephalography (EEG) to systematically investigate the time course underlying aspect ratio, animacy, and category information during visual object processing. Participants (N = 20) viewed the stimulus set used by Yargholi and Op de Beeck (2023), as well as silhouette versions of the stimuli that lacked internal object details (thus increasing reliance on shape information). Stimuli appeared in 5 Hz rapid serial visual presentation streams, with intact and silhouette stimuli sets shown in separate streams. Using standard multivariate decoding pipelines and representational similarity analysis, we found that information about aspect ratio, category, and animacy was represented during visual object processing. The dominant dimension was modulated by stimulus type, demonstrating that the observable dimensions of object space depend on the nature of the stimuli presented. Taken together, these findings demonstrate that aspect ratio is indeed represented during object processing, but earlier and more transiently than categorical dimensions, such as animacy. By focusing on underlying temporal dynamics, our results provide a more nuanced understanding of how object space evolves over time that can speak of how extant findings on this topic might be reconciled.

Keywords: EEG, object space, object processing, temporal dynamics

1. INTRODUCTION

The human visual system is highly skilled at rapidly and accurately recognizing a wide range of visual stimuli. However, the overarching organizational principles used by the visual system to represent these objects are still debated. Several dimensions have been proposed to underlie the organization of object space. These dimensions span a continuum from low-level visual statistics (Coggan et al., 2016; O'Toole et al., 2005; Rice et al.,

2014) and mid-level properties, such as shape (Bracci & Op de Beeck, 2016; Kayaert et al., 2005; Nasr et al., 2014) and size (Huang et al., 2022; Konkle & Caramazza, 2013; Konkle & Oliva, 2012), to higher level characteristics, such as animacy (Kriegeskorte et al., 2008; Sha et al., 2015), categorical information (Kriegeskorte et al., 2008), humanness (Contini et al., 2020; Grootswagers et al., 2022), agency (Thorat et al., 2019), and semantic information (Chao et al., 1999; Naselaris et al., 2009). While these diverse features are all represented during

Received: 19 November 2024 Revision: 12 September 2025 Accepted: 14 November 2025 Available Online: 20 November 2025



The MIT Press

© 2025 The Authors. Published under a Creative Commons Attribution 4.0 International (CC BY 4.0) license.

Imaging Neuroscience, Volume 3, 2025
<https://doi.org/10.1162/IMAG.a.1051>

object processing, it is still unclear which dimensions primarily drive neural responses, and how these dimensions can best be explained by a unified model of object space.

Recently, a comprehensive map of object space in macaque inferior temporal (IT) cortex was proposed (Bao et al., 2020). This map is characterized by two orthogonal dimensions in which objects can be distributed: the animate–inanimate dimension (animacy) and the stubby–spiky dimension (aspect ratio) (Bao et al., 2020). This map was repeated three times across the hierarchical stages of the ventral visual stream as object representations increased in view invariance. When investigating whether this model also exists in humans, representations of and selectivity for all four quadrants of this proposed space (stubby–animate, stubby–inanimate, spiky–animate, spiky–inanimate) were found using 7T functional magnetic resonance imaging (fMRI) (Coggan & Tong, 2023). However, the functional organization found in humans did not mirror the functional organization found in macaques. The stubby–animacy map selectivity highly overlapped with areas traditionally considered selective to different categories (such as face- and body-selective regions), and there were no clear repetitions across hierarchical stages of the visual stream, indicating that while animacy and aspect ratio were fundamental organizing principles, there were differences between the macaque and human visual systems (Coggan & Tong, 2023).

A critique of this map of object space is that the stimuli that were primarily used to identify the aspect ratio and animacy axes did not control for category (Yargholi & Op de Beeck, 2023). In both studies, the stimulus set confounded category and aspect ratio, in that faces were only represented in the stubby–animate quadrant and bodies primarily belonged in the spiky–animate quadrant of object space. To investigate object space and the anatomical distribution of aspect ratio in human visual systems, Yargholi and Op de Beeck (2023) conducted an fMRI study that used a new stimulus set that dissociated category from aspect ratio. In contrast to Bao et al. (2020), these authors observed comparatively limited tuning for aspect ratio (stubby vs spiky) in object-selective areas, but strong evidence for both category and animacy representations in these regions. A small effect of aspect ratio was observed in right Fusiform Gyrus-object and right Lateral Occipital Complex-object, and aspect ratio information of inanimate objects was represented in regions of object-selective cortex. However, when including animate stimuli, aspect ratio was not an encompassing dimension. In contrast, early visual areas, such as V1 more strongly represented information about aspect ratio (Yargholi & Op de Beeck, 2023). Therefore, while the authors concluded that some aspect ratio information is available in occipitotemporal cortex, aspect ratio likely

does not have a special status for the large-scale organization of object space, and that functional organization of the human ventral visual stream is primarily driven by the dimensions of category and animacy (Yargholi & Op de Beeck, 2023).

What accounts for these contradictory findings? While the use of different stimulus sets may have contributed in part, it seems likely that the different neuro-imaging techniques utilized by the studies may play an important role. In the original macaque study, the stubby–spiky networks were initially found using electrophysiology, whereas fMRI was used in both human studies (Bao et al., 2020; Coggan & Tong, 2023; Yargholi & Op de Beeck, 2023). It is possible that aspect ratio is used earlier and more transiently than animacy and category information, and due to the slow hemodynamic response, fMRI may not be able to pick up on this dimension as strongly when compared with millisecond-resolution electrophysiology. Additionally, the dimensions that support object processing may be flexible, in that dimensions are weighted differently depending on the object's available visual information. The macaques viewed “silhouette” objects in conjunction to objects with preserved internal details (Bao et al., 2020), while the human participants only viewed objects with preserved internal details (Coggan & Tong, 2023; Yargholi & Op de Beeck, 2023). In conjunction to the varying levels of object detail available in these studies, macaques were shown several objects that they did not have familiarity with (e.g. camera, wheelchair, musical instruments), whereas human participants had category and experiential knowledge about all presented stimuli. Aspect ratio may be used more strongly for objects for which category information is not obvious, or for stimuli that only have silhouette information available, in comparison with known objects that have internal details easily accessible to the visual system. Comparing representations of silhouette stimuli with their intact counterparts in human participants could bridge this gap in the literature, and provide data on how dimensions of object space be differently represented depending on stimulus information available at a certain time.

The goal of the present study was to address these possibilities by using electroencephalography (EEG) and multivariate pattern analysis (MVPA). Because EEG has a high temporal resolution, it may be more sensitive to object space representations that occur or evolve quickly than fMRI techniques. Using rapid serial visual presentation (RSVP), we presented the stimulus set that dissociated aspect ratio from category, along with the silhouette version of the same stimuli, to human participants in order to directly compare the impact of masking internal features on the object space dimensions used during

object processing (Yargholi & Op de Beeck, 2023). Our results indicated that aspect ratio was indeed represented during object processing, however, this information was available earlier, more transiently, and less strongly in comparison with animacy and category information for objects with internal details. However, masking object details via silhouettes strengthened aspect ratio information, which became the primary dimension represented, while concurrently weakening animacy and category information. These findings provide insights from a temporal perspective on the functional model underlying object space, and indicate that the dimensions used during object processing are influenced by the visual information we have access to.

2. METHODS

2.1. Participants

Twenty-two healthy individuals with normal or corrected-to-normal vision volunteered to participate in the study. Participants were recruited from the undergraduate student population and the Western Sydney community. Two participants were excluded due to incomplete recordings, and the data from the remaining 20 participants (13 female, mean age 23.65 years, SD = 4.04) were included in all analyses. All participants had normal or corrected-to-normal vision. The study was approved by the Western Sydney University Institutional Review Board, and informed consent was obtained from all participants before the start of the experiment.

2.2. Stimuli

We used the original stimulus set from Yargholi and Op de Beeck (2023), consisting of 52 object stimuli across 4 categories: bodies, faces, manmade objects, natural (Yargholi & Op de Beeck, 2023; Fig. 1A). There were 13 stimuli within each category, 6 of which had small aspect ratios and were, therefore, classified as “stubby,” 6 with large aspect ratios (classified as “spiky”), and 1 that represented the median aspect ratio in that category. Aspect ratio was defined as $P^2/(4\pi A)$, where P represented the perimeter of the object, and A was the area of the object. All images were grayscale, covered 6.5 x 6.5 degrees of visual angle, and were presented on a light gray background. The luminance and average energy at each spatial frequency across these images were equalized (Yargholi & Op de Beeck, 2023). This stimulus set is referred to as the “intact” stimuli in our paradigm.

To examine how available stimulus information modulates neural representations of object space, we included silhouette versions of all stimuli. By masking each object’s

internal features, silhouettes of the object stimuli effectively degrade category object information while leaving aspect ratio information untouched (Quek et al., 2025). Images were binarized using custom code in Matlab. All pixels belonging to the stimulus image were assigned the value of 0.2 and appeared dark gray. These images were also 256 x 256 and were presented on a gray background. All participants viewed both the intact stimuli and the silhouette version of each stimulus, for a total of 104 stimuli included in the study (Fig. 1A).

2.3. Paradigm

Stimuli were presented at a rate of 5 Hz (200 ms/image) in a continuous stream using a rapid serial visual presentation (RSVP) paradigm (Grootswagers, Robinson, & Carlson, 2019; Grootswagers, Robinson, Shatek, et al., 2019; Peirce et al., 2019; Robinson et al., 2019). In several previous studies, RSVP has successfully been used in combination with multivariate pattern analysis to decode both individual images and higher-order visual information, such as category representations (Grootswagers, Robinson, & Carlson, 2019; Grootswagers et al., 2022, 2024, 2025; Grootswagers, Robinson, & Carlson, 2019; Robinson et al., 2019, 2025; Shatek et al., 2022). The signal from the presented stimulus is distinguishable from the average visual signal evoked by other stimuli presented before and after the stimulus of interest for each trial. This design made sure that stimuli before and after the presented stimulus were not systematically different, ensuring these neural signals did not impact decoding results. Each run consisted of a randomized stream of 208 object stimuli (4 repeats of each stimulus), and silhouette images and intact images were always presented in separate runs (Fig. 1B). The order the stimuli were presented in was yoked across the intact and silhouette images, so that there were no differences in the presentation order for the different stimulus types. Participants were instructed to fixate on an overlayed center point on the screen, and completed an orthogonal task in which they pressed a button when seeing a target shape of a square or triangle (Fig. 1B). There were two to four target shapes in each run. Runs lasted between 42 and 42.4 s, and each participant completed a total of 40 runs of this task (20 runs of the intact stimulus set, and 20 runs of the silhouette stimuli). These yoked runs were presented in a randomized order for all participants, such that all stimuli were equally likely to precede and follow every other stimulus. Every stimulus was presented 80 times, for a total of 8,320 (excluding targets) trials during the experiment. The experiment was coded in Python (v 3.6.6.) using the Psychopy library (Peirce et al., 2019). Before starting the experiment, participants completed a

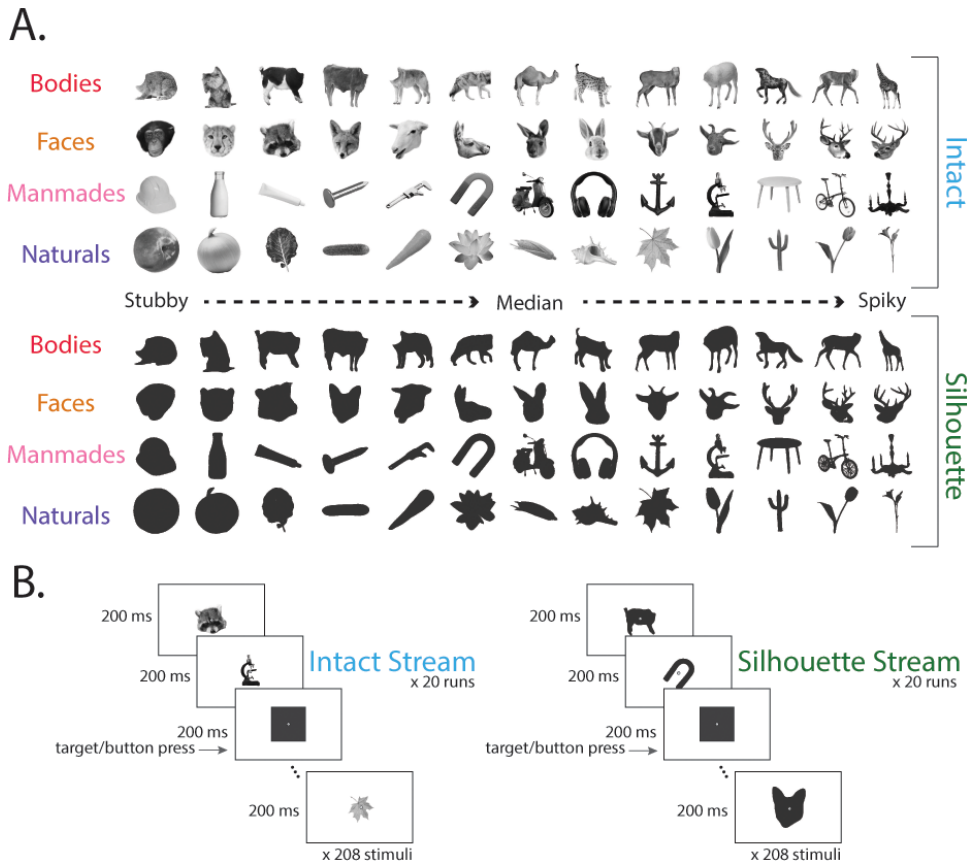


Fig. 1. EEG stimuli and experimental design. (A) Visual stimuli used in this experiment included “intact” stimuli (obtained from [Yargholi & Op de Beeck, 2023](#)) and silhouette versions of those same stimuli. This stimulus set dissociated animacy from aspect ratio, so that within each category, half of the stimuli were stubby while the other half were spiky. (B) Schematic example of an intact and silhouette stimulus run. Participants fixated on central cross while completing an orthogonal task (press the button when a triangle or square appeared).

practice run to familiarize themselves with the speed of stimuli presentation and the task.

2.4. EEG acquisition and preprocessing

Data were continuously recorded using a 64-channel Biosemi system at a sampling rate of 2048 Hz. Impedance was reduced below 25 kOhm at each electrode site whenever possible using conductive gel. We used a 64-channel electrode system, arranged according to the international standard 10-10 system. All stimuli were presented on a Viewpixx 120 Hz monitor, and a trigger was sent for the onset of a run, the onset of each stimulus, and the offset of each stimulus.

Minimal preprocessing was performed using the Fieldtrip (version 20231015; [Oostenveld et al., 2011](#)) in MATLAB (version R2022b; The Mathworks, Natick, MA). Data were downsampled to 200 Hz and demeaned to 100 ms before stimulus onset ([Grootswagers et al., 2017](#)). Epochs of -100 to 800 ms relative to stimulus onset were created for each trial. No additional preprocessing was performed.

2.5. Multivariate analysis

All following analyses were performed using functions from the CoSMoMVPA toolbox ([Oosterhof et al., 2016](#)), and custom code in MATLAB (version R2022b; The Mathworks, Natick, MA). We took a multivariate approach to the data ([Grootswagers et al., 2017](#)). To determine whether representations of aspect ratio, animacy, and category were present for objects in whole-brain EEG signal, we performed classification analysis. Next, to examine the temporal dynamics and stability of each dimension of object space, we ran a temporal generalization analysis ([King & Dehaene, 2014](#)). To test which feature dimension best represented the data across time points, we used representational similarity analysis (RSA) and compared model representational dissimilarity matrices (RDMs) with RDMs generated by the EEG data.

2.6. Classification analysis

A regularized linear discriminant analysis (LDA) classifier was trained to decode between whole-brain patterns in

the EEG signal across all electrodes at each time point of the trial. Classifiers were trained to decode between separate conditions (stubby vs. spiky, animate vs. inanimate, category, individual stimulus) using a leave-one-run-out cross-validation approach. Silhouette stimuli and intact stimuli were analyzed separately from one another. When decoding stubby vs. spiky, the object stimuli that were the median for each category were removed from analysis, as they were classified and neither stubby or spiky. The resulting chance-level accuracy was 50% for the classification of animacy and aspect ratio, 25% for stimulus category, and 1.92% for individual stimulus identity (52 images). This classification was performed for each participant individually, and then averaged across participants to obtain the mean classification accuracy across individuals.

2.7. Sensor searchlight classification analysis

To investigate the spatial distribution of dimension information, we performed a sensor searchlight analysis. A regularized LDA classifier was trained at each time point of the trial on neighborhoods of four sensors. As in the whole-head classification analysis above, these classifiers were trained to discriminate between separate conditions (stubby vs. spiky, animate vs. inanimate, category) and silhouette and intact stimuli were analyzed separately from one another. The resulting chance-level accuracies were the same as in the whole-head classification analysis for each dimension. This classification was performed for each participant individually and then averaged across participants to obtain the mean classification accuracy across individuals. For the purpose of displaying these results, we then averaged each dimension's decoding accuracies across 100 ms time bins, beginning at 50 ms before stimulus onset.

2.8. Cross-decoding classification analysis

Next, we evaluated how well representations of aspect ratio could generalize across changes in other object dimensions, such as animacy information. To do so, we conducted a cross-decoding analysis on whole-brain EEG patterns between the dimensions of aspect ratio and animacy, as has been performed in related object processing literature (Yargholi & Op de Beeck, 2023). This analysis was similar to the previous classification analysis, except the training and testing sets were separated according to the other dimension. Specifically, a regularized LDA classifier was trained to distinguish the classes within a given dimension (e.g., animate vs. inanimate) using only the trials from one class of stimuli within the other dimension (e.g., training set limited to stubby stim-

uli). The LDA classifier was then tested using trials from the held-out class of stimuli (e.g., test set limited to spiky stimuli). We then repeated the analysis reversing the train/test sets, and averaged the results of the two analyses. This analysis was conducted at every time point of the trial. A leave-one-run-out cross-validation approach was used, and silhouette and intact stimuli were analyzed separately from one another. The resulting chance-level accuracy was 50% for both aspect ratio and animacy decoding. Once again, this classification was performed for each participant individually and then averaged across participants, resulting in the mean classification accuracy across individuals.

2.9. Temporal generalization analysis

We performed a temporal generalization analysis to determine the stability of the representations of different dimensions of object space (Carlson et al., 2011; King & Dehaene, 2014). This analysis tested whether the representational structure of each dimension was consistent across time points, or whether there were shifts in this representation over the time course of object perception. LDA classifiers were trained to discriminate between conditions at each time point and then were tested at all other time points.

2.10. Representational similarity analysis

To find the feature model that best fit the EEG data at each time point, representational similarity analysis (RSA) was implemented (Kriegeskorte, Mur, & Bandettini, 2008). RSA is a multivariate computational technique that compares the similarity of neural representations of different stimuli by using similarity or distance matrices. These matrices can then be interpreted based on patterns of similarity, or used to test models that represent how neural data would be organized if that model drove similarity between stimuli. In this study, to characterize the similarity between each stimulus within whole-brain EEG responses, an LDA classifier was trained to discriminate between each stimulus pair at each time point (i.e. pairwise decoding), and the resulting values were placed into representational dissimilarity matrices (RDMs). Intact and silhouette stimuli were analyzed separately. Next, model RDMs were created for aspect ratio and category. We focused on these two dimensions because category and aspect ratio have been proposed to explain one another in the literature (Bao et al., 2020; Yargholi & Op de Beeck, 2023). In these model RDMs, stimuli pairs that were predicted to be similar were given values of 0 (e.g. two spiky stimuli in the aspect ratio model), and stimuli that were predicted to be different were given values of 1 (e.g. one

stubby and one spiky in the aspect ratio model). We also included a pixel-level model that captures pixel information. The pixel models were made separately for intact and silhouette stimuli and were generated using the pairwise Jaccard distance between pixel values in each stimulus. This identified the amount of pixel overlap between all object images. To determine which model best explained the representational structure of the neural data, a linear model was then conducted at each time point of the trial, resulting in a beta value at every time point in the trial. Linear models were performed separately for intact and silhouette stimuli. This analysis resulted in a time course of beta values in which the beta value can be interpreted as the strength of that model's ability to predict the neural data.

2.11. Statistical analysis

To test the probability of above-chance (alternative hypothesis) classification versus chance-level (null hypothesis) classification across participants at each time point, we conducted Bayes Factors (Teichmann et al., 2022). This analysis allowed us to directly assess and measure the strength of different hypotheses. Bayes Factors were calculated using the Bayes Factor R package (Morey et al., 2015) implemented in Matlab (Teichmann et al., 2022). Bayesian t-tests were run at each time point. To allow for small effects under the alternative hypothesis, the prior range of the alternative hypotheses was two-tailed, from -infinity to -0.5 and from 0.5 to infinity (Rouder et al., 2009). By using a two-tailed prior range, we could better capture strength of evidence for any below-chance decoding, compared with one-tailed priors. A half-Cauchy prior with the default, medium width of 0.707 was used (Teichmann et al., 2022). Larger Bayes Factors (BFs) indicate more evidence for the alternative hypothesis that there is above-chance classification. Specifically, BFs that are larger than 1 are evidence for above-chance decoding, whereas Bayes Factors smaller than 1 support at-chance decoding. The strength of Bayes Factors is directly interpretable, such that a BF of 5 indicates that the observed data are five times more likely under the alternative hypothesis compared with the null hypothesis, whereas a Bayes Factor of 1/5 indicates that observed data are five times more likely under the null hypothesis compared with the alternative hypothesis. This Bayesian approach was implemented for the classification and temporal generalization analysis. A similar Bayesian method was also used to compare neural RDMS to model RDMS at each time point, however, the prior range was adjusted to be two-tailed without an expected null prior value.

Additionally, Bayes Factors were used to evaluate the probability of above-chance differences in decoding,

temporal generalization, and beta values between intact and silhouette stimuli for each dimension. Within each participant, we calculated the difference between decoding accuracy (for both the decoding analysis and temporal generalization analysis) and beta values for intact and silhouette stimuli at each time point and performed Bayesian t-tests against 0. We used a half-Cauchy prior with the default, medium width of 0.707 (Teichmann et al., 2022), and we excluded the interval between $d = -0.5$ and $d = 5$ from the prior. Bayes Factors corresponding to differences between intact and silhouette stimuli are included in each figure for decoding, temporal generalization, and RSA.

3. RESULTS

3.1. Decoding analyses demonstrate unique temporal dynamics underlying representations of each object space dimension

To investigate the temporal dynamics underlying the dimensions of aspect ratio, animacy, and category during object processing, we trained separate linear classifiers to discriminate aspect ratio (stubby vs. spiky), category (faces vs. bodies vs. manmade objects vs. natural objects), and animacy (animate vs. inanimate). These analyses were carried out separately for intact and silhouette stimuli and resulted in a time series of decoding accuracies that revealed when information related to each dimension was decodable for each stimulus type (Fig. 2).

Each dimension was decodable in both intact and silhouette stimuli, and decoding onset was similar across all dimensions for both stimulus types. In both intact and silhouette stimuli, aspect ratio (stubby vs. spiky) decoding peaked ~93 ms after stimulus onset, which was earlier than both animacy and category information (peak decoding at ~118 ms and ~125 ms, respectively). While each dimension had a second decoding peak in both intact and silhouette stimuli, this peak had lower accuracy for aspect ratio, whereas the second decoding peak was as accurate or had a higher accuracy than the initial decoding peak for both animacy and category. Above-chance decoding was sustained after stimulus offset for each dimension. In both stimulus types, aspect ratio decoding offset occurred ~500 ms after stimulus onset, animacy decoding offset occurred ~525 ms after stimulus offset, and category decoding offset occurred ~550 ms after stimulus onset.

Importantly, the decodability of each dimension was modulated by the amount of available stimulus information. Aspect ratio decoding was more accurate for silhouette stimuli (peak decoding ~63%) than for intact stimuli (peak decoding ~57%) during stimulus presentation, and strong evidence for an above-chance difference in

decoding strength began before the initial decoding peak at ~65 ms until ~145 ms after stimulus onset (Fig. 2A). This pattern was reversed for both animacy and category decoding (Fig. 2B, C). Decoding accuracy was higher for both dimensions in intact stimuli (animacy decoding accuracy at ~61.5% and category decoding accuracy at ~35.5%) than silhouette stimuli (animacy decoding accuracy at ~56% and category decoding accuracy at ~31%). Evidence for above-chance differences in decoding strength occurred later (both occurring around 100 ms after stimulus onset) and for a more sustained period of time (including after the stimulus was no longer on the screen) for category and animacy when compared with the aspect ratio dimension.

To investigate the spatial topography of these decoding results, we also performed a sensor searchlight analysis for each object space dimension (Fig. 2). Overall decoding accuracies were lower in this analysis than in whole-head EEG decoding. Across each dimension, the general distribution of information over the sensors was largely similar. Above-chance decoding was primarily observed in posterior occipital sensors, especially during 50–150 ms post-stimulus presentation. After the initial decoding peak, information was available over more sensors, moving anteriorly along occipital and temporal sensors. Similarly to the whole-head EEG results, the strength of decoding in the sensors was modulated by available stimulus information. Aspect ratio decoding accuracies were stronger for silhouette stimuli than for intact stimuli, and vice versa for category and animacy decoding.

These decoding results indicate that the dimensions of aspect ratio, animacy, and category have different temporal dynamics from one another, but similar spatial topographies. Aspect ratio information is available earlier

and for a shorter time period than category and animacy, and available stimulus information directly impacts the amount of information available for each dimension underlying object space.

3.2. Cross-decoding analyses show generalizability in object space dimensions of aspect ratio and animacy

Next, to investigate how signals related to aspect ratio could generalize across changes in other object space dimensions, and vice versa, we conducted a cross-

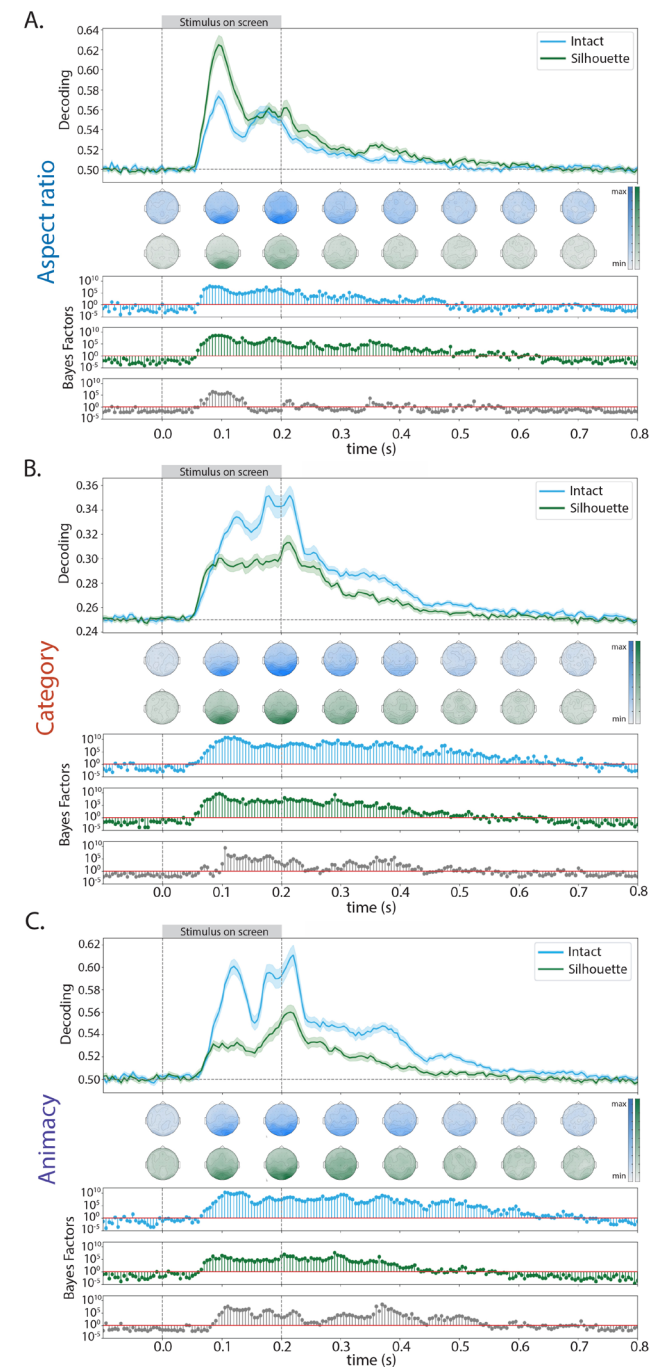


Fig. 2. Mean decoding accuracy from whole-head EEG activation patterns for decoding. (A) The aspect ratio (stubby vs. spiky) of the object, (B) the category (face, body, manmade object, natural object) of the object, and (C) the animacy (animate vs. non-animate) of the object. In all plots the shaded region indicates the standard error at that time point. Directly below the mean decoding accuracies are topoplots showing sensor searchlight results (blue for intact stimuli and green for silhouette stimuli) averaged across 100 ms time bins. The corresponding Bayes Factors for decoding of each stimulus type are then below the searchlight plots. Bayes Factors for the difference (intact–silhouette) between decoding accuracy in the intact stimuli and silhouette versions of those stimuli and included in gray. Information about each object space dimension was available in intact and silhouette stimuli, and decoding strength of each dimension was modulated by stimulus information available. The distribution of information across sensors is similar for each dimension of object space, and between intact and silhouette stimuli.

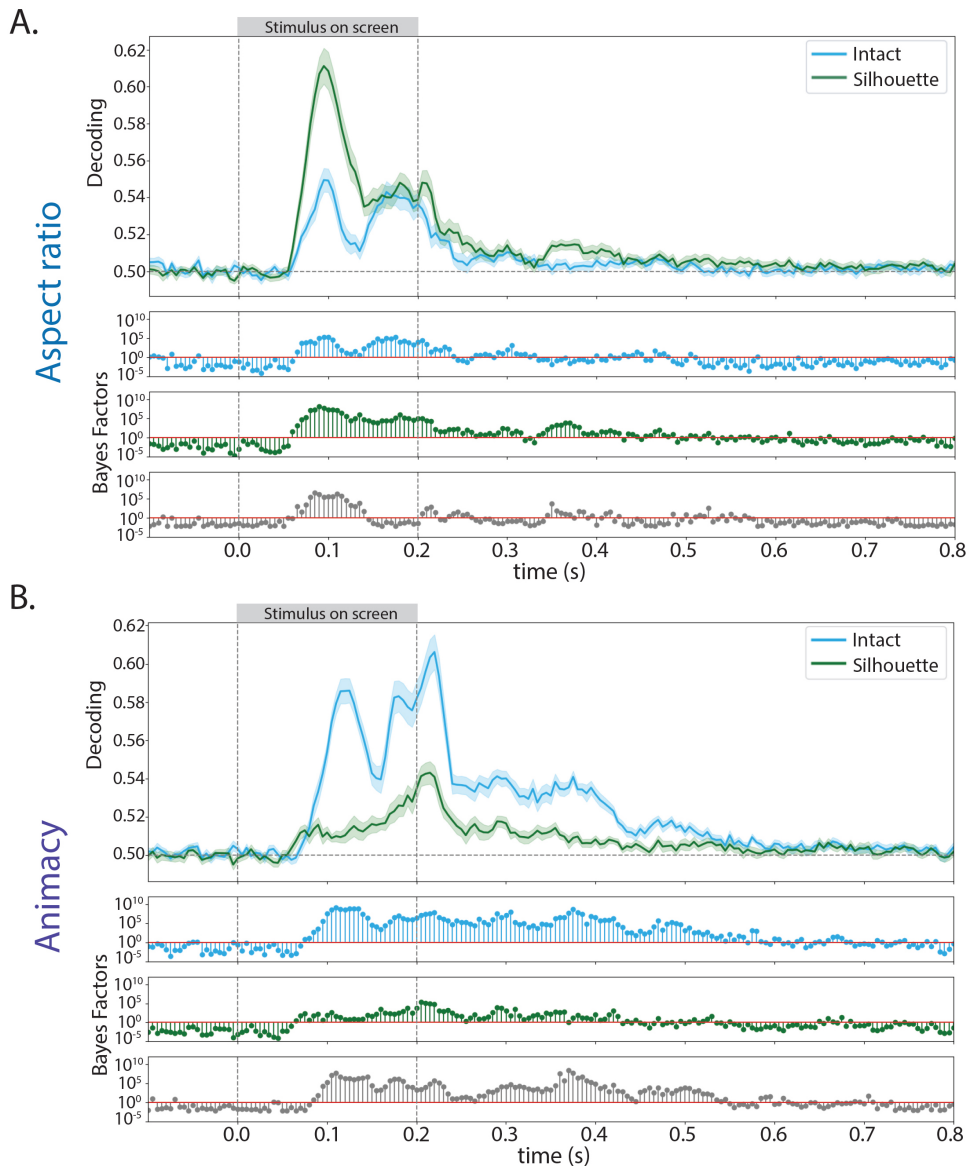


Fig. 3. Mean cross-decoding accuracies from whole-head EEG activation patterns for decoding. (A) Aspect ratio (stubby vs. spiky) of an object and (B) animacy (animate vs. inanimate) of an object. In each plot, the shaded region indicates the standard error at that time point. Directly below the mean decoding plots are the corresponding Bayes Factors for that time point (blue for intact stimuli and green for silhouette stimuli). Bayes Factors for the difference (intact–silhouette) between decoding accuracy in the intact stimuli and silhouette versions of those stimuli and included in gray. Both object space dimensions showed above-chance decoding, demonstrating that this information is generalized across changes in the other dimension.

decoding classification analysis. In line with the literature (Yargholi & Op de Beeck, 2023), we trained classifiers on animate stimuli to distinguish between stubby and spiky stimuli and then tested the classifier on inanimate stimuli (and vice versa). Classifiers were also trained to distinguish between animate and inanimate stimuli using stubby objects, and then tested on spiky objects (and vice versa). This resulted in classification accuracies at every time point of the trial, elucidating when information was generalizable across object space dimensions (Fig. 3).

In line with our decoding results, cross-decoding of animacy was stronger in the intact stimuli whereas

cross-decoding of aspect ratio was stronger in the silhouette stimuli. Both object space dimensions of aspect ratio and animacy were decodable during this cross-decoding classification in intact and silhouette stimuli. Aspect ratio decoding peaked around 95 ms post-stimulus onset for both intact and silhouette stimuli, and decoding was stronger in silhouette stimuli. Animacy decoding showed different temporal dynamics when compared with aspect ratio. In intact stimuli, animacy decoding peaked ~115 ms after stimulus onset, and then remained significantly above-chance decoding until about 340 ms after the stimulus was no longer on the

screen. In silhouette stimuli, above-chance decoding occurred for the entirety of the stimulus being on the screen, beginning around 60 ms. However, peak decoding did not occur until after the stimulus was off the screen (~215 ms post-stimulus onset, or ~15 ms post-stimulus offset). These results demonstrate that signals related to aspect ratio and animacy generalize across objects of different animacy and aspect ratio, respectively. This generalization occurs both during stimulus presentation and after the stimulus is no longer shown, and is modified by stimulus information available to the visual system.

3.3. Temporal generalization analysis shows different patterns of information stability across object space dimensions, which is directly modulated by available stimulus information

To evaluate the stability of each dimension over time, temporal generalization analysis was performed. We trained and tested classifiers on different time points

during the trial, resulting in a measure of information generalization during and after stimulus presentation. Off-diagonal classification indicates that information is transiently represented over those time points, whereas classification that looks like a square near the diagonal, or classification found in the upper or lower triangle of the graph, suggests information stability across time.

Once again, different temporal dynamics were observed for aspect ratio in comparison with animacy and category (Fig. 4). Almost no generalization was found for aspect ratio in intact stimuli, and no above-chance classification occurred after 500 ms post-stimulus onset (Fig. 4A). In silhouette stimuli, above-chance generalization occurred beginning ~86 ms after stimulus onset, and remained after stimulus offset. Additionally, there was off-diagonal generalization, in which early time points between 86 ms and 185 ms post-stimulus onset generalized through 600 ms after stimulus offset (Fig. 4B). This pattern indicates that aspect ratio information is more transiently available during visual processing of the intact stimuli, and for silhouette object stimuli, aspect ratio information is held consistently

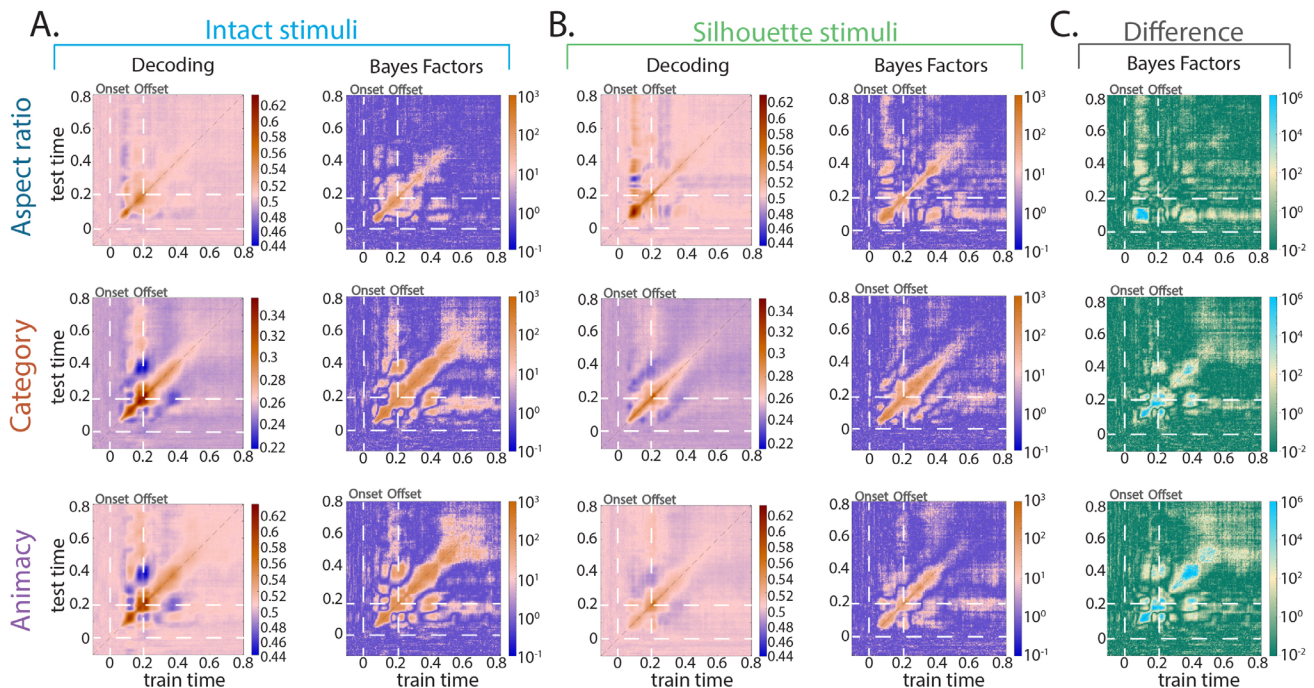


Fig. 4. Mean temporal generalization for decoding each dimension in (A) the intact stimuli and in (B) silhouette stimuli. For all decoding plots, pink indicates chance-level temporal generalization decoding accuracy values, while warm orange-red indicate above-chance decoding accuracy values and blue indicates below-chance decoding. (C) The Bayes Factors corresponding to the difference in temporal generalization decoding accuracy for each dimension between intact and silhouette stimuli. For Bayes Factors plots in (A) and (B), warm colors (pink and light-to-dark orange) indicate Bayes Factors above 1 (evidence for the alternative hypothesis), while blue indicates Bayes Factors below 1 (evidence for the null hypothesis). For Bayes Factors plots in (C), yellow and light blue indicate Bayes Factors above 1 (evidence for the alternative hypothesis), while green indicates Bayes Factors below 1 (evidence for the null hypothesis). The points along the diagonal of each plot represent testing and training on the same time point. In the intact stimuli, stability in category and animacy information was observed, while in the silhouette stimuli, stability in aspect ratio (stubby vs. spiky) information was observed. Strong evidence for above-chance differences between temporal generalization in the intact stimuli and the silhouette stimuli for each dimension was found.

over time. In contrast, generalization of animacy and category information over time was found during object processing of the intact stimuli (Fig. 4A). Above-chance animacy classification began around 90 ms after stimulus onset, and again around 180 ms after stimulus onset through to 35 ms after stimulus offset. Small, but above-chance, generalization also occurred between ~300 ms and ~550 ms after stimulus offset. Off-diagonal classification was found between the time points of ~200 ms and ~550 ms after onset. Category classification had almost the exact same pattern of generalization, and off-diagonal decoding was found for multiple periods of time during and after stimulus presentation in the intact stimuli data (Fig. 4B). There was almost no evidence for above-chance off-diagonal classification, apart from weak classification between ~480 ms and 600 ms after stimulus offset. These results re-enforce that aspect ratio has differential temporal dynamics from category and animacy. Additionally, these data support that the amount of stimulus information available does not only impact when object space dimensions are represented in the neural signal, but also the stability of that representation over time. For all dimensions, evidence for above-chance differences between the temporal generalization accuracies in the intact stimuli and the silhouette was observed (Fig. 4C). Below-chance decoding was observed for temporal generalization of each dimension, primarily and most strongly when the training or testing time point was around time of stimulus offset (Fig. 4A and 4B). This below-chance decoding has been observed in previous studies (Carlson et al., 2014; Cichy et al., 2014), and has been suggested to be caused by visual responses to stimulus offset (Carlson et al., 2014).

Overall, these results indicate that aspect ratio information is more transiently represented than category and animacy information in stimuli in which internal details are preserved. However, this pattern is reversed in the silhouette stimuli, mirroring the decoding results. In stimuli without internal details, aspect ratio information is more strongly represented and is more stable than animacy and category information.

3.4. Representational similarity analysis demonstrates aspect ratio and category information uniquely explain EEG whole-brain neural patterns, even when including a model representing pixel-level object information

Lastly, to examine which object space dimension best explains the representational structure of the neural data, and whether pixel-level information can explain the neural data differently than object space dimensions, we performed a linear model between the neural representational dissimilarity matrix and model dissimilarity matrices rep-

resenting aspect ratio, category, and pixel information at each time point (Fig. 5). This resulted in a time course of beta values at every time point, which can be interpreted as the relative strength that model explains the observed neural data, while taking into the other model into consideration. We chose to focus on aspect ratio and category object space dimensions in this analysis, because conflicting results were found for these dimensions in previous proposed maps of object space (Bao et al., 2020; Coggan & Tong, 2023; Yargholi & Op de Beeck, 2023). We also performed this analysis when including a model representing animacy and the results were largely preserved as they are reported here.

The aspect ratio model explained the neural data best for both intact and silhouette stimuli beginning around 70 ms and peaked around 95 ms after stimulus onset (Fig. 5). For intact stimuli (Fig. 5A), the category model then best explained the neural data beginning around 110 ms after stimulus onset for the rest of the time the stimulus was on the screen until ~225 ms after stimulus offset. The aspect ratio model uniquely explained the neural data throughout the trial as well until approximately 20 ms after stimulus offset. The pixel model uniquely explained the neural data in intact stimuli consistently between ~140 ms after stimulus onset until ~10 ms after stimulus offset. In contrast, there was no evidence that the category model explained the neural data for silhouette stimuli at almost any point in the trial (briefly for ~25 ms after stimulus offset) (Fig. 5B). Instead, aspect ratio information best explained the neural signal until ~120 ms after stimulus onset, and uniquely explained variance in the neural data until 200 ms after stimulus offset. The pixel model did explain some of the neural variance in silhouette stimuli as well, beginning ~105 ms after stimulus onset. It best explained the data beginning ~150 ms after stimulus onset, however, had overall weaker Bayes Factors than the aspect ratio model during and after stimulus presentation.

Bayes Factors showed strong evidence for differences between the betas in the intact stimuli and silhouette stimuli (Fig. 5C) for the aspect ratio, category, and pixel models. These differences primarily occurred earlier for the aspect ratio model and occurred more consistently later in the trial, including after stimulus offset, for the category and pixel models. These data suggest that both aspect ratio and category information explain unique components of the neural signal when viewing intact and silhouette objects. Category information better explains the neural data for a longer period of time in the intact stimuli, however, does not explain the neural data at almost any point in the silhouette stimuli. Moreover, these results demonstrate aspect ratio and category information cannot be solely explained by pixel information.

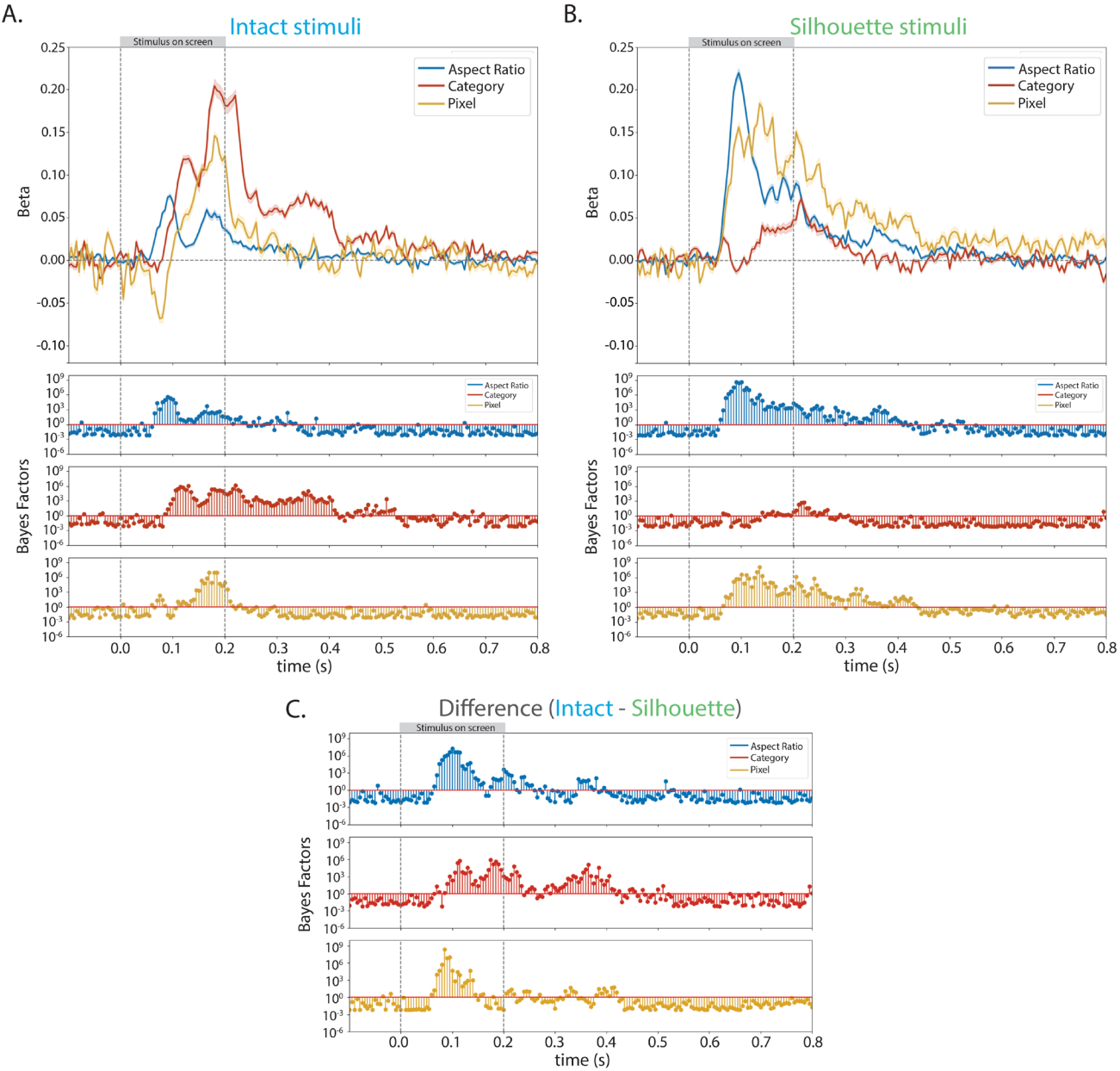


Fig. 5. Mean beta values corresponding to models of aspect ratio, category, and pixel calculated via linear models in (A) intact stimuli and (B) silhouette stimuli. In all plots, the shaded region indicates the standard error at that time point, and the corresponding Bayes Factors for each stimulus type (blue for intact stimuli and green for silhouette stimuli) are directly below the betas plot. (C) Bayes Factors for the difference (intact–silhouette) between beta values in the intact stimuli and silhouette versions of those stimuli during the entire trial. The category model better explained the representational structure of the neural data for the intact stimuli, and the aspect ratio model better explains the representational structure of the neural data for the silhouette stimuli. The pixel model does not explain the data better than the dominant object space dimension. Moreover, even when including the pixel model in the linear model, both aspect ratio (stubby vs. spiky) and category information still uniquely explain the neural data during visual object processing.

4. DISCUSSION

The goal of this experiment was to evaluate whether, and when, representations of proposed object space dimensions were available during visual processing of intact object stimuli and object stimuli with masked internal details. Specifically, we investigated the temporal dynam-

ics of aspect ratio, category, and animacy representations using multivariate pattern analysis of whole-head EEG signals. We found that representations of each dimension were available in the neural responses to both stimulus types. Overall, aspect ratio information was available earlier than category and animacy information, and the

strength of decoding was modulated by stimulus information available during visual processing. Specifically, decoding and cross-decoding of animacy were stronger in intact stimuli, whereas decoding and cross-decoding of aspect ratio were stronger in the silhouette stimuli. Aspect ratio information was also more transiently available than category and animacy information in the intact stimuli, both of which were stable over time. However, in silhouette stimuli, aspect ratio information was more stable than category and animacy information. Models of aspect ratio and category object information differentially explained the representational structure of the neural data over time in the intact stimuli, and aspect ratio best explained the neural data in the silhouette stimuli during periods of the stimulus presentation, even when including a model representing pixel information. Overall, these results demonstrate that each dimension of object space has distinct temporal dynamics, and the amount of stimulus information available during visual object processing directly modulates the representations of these dimensions over time. Importantly, our findings highlight the significance of considering temporal information when defining object space (Robinson et al., 2023).

The fundamental organizing principles of object space and higher order visual regions have been the subject of several studies and debates. For example, a model of object space in macaque inferotemporal cortex was recently proposed, defined by orthogonal dimensions of aspect ratio and animacy (Bao et al., 2020). This model accounted for category information (e.g. face and body representations) as a result of the four quadrants of this two-dimensional object space. Some evidence for these organizing principles was found in human inferotemporal cortex, however, a clear sequence of this object space was not observed, and the selectivity of aspect ratio–animacy space highly overlapped with category selectivity (Coggan & Tong, 2023). When using a stimulus set that dissociated category and aspect ratio information, object space and the organization of human occipitotemporal cortex were better characterized by the dimensions of category and animacy. In this model, aspect ratio was not as strongly represented, and this dimension was instead better explained by category and animacy effects (Yargholi & Op de Beeck, 2023). These diverging conclusions could be a result of the different stimulus set, different amounts of category information available between species (e.g. object category familiarity), or the lack of temporal sensitivity in human fMRI compared with macaque electrophysiology data. Our results directly speak of these possible explanations. First, we used the stimulus set that dissociated aspect ratio and category information and created a silhouette version of those stimuli, effectively masking internal stimulus details and reducing available category

information. Secondly, we used EEG to evaluate changes over fine-grained periods of time during object processing. Information about aspect ratio is strongest in the neural response to our stimuli ~100 ms after stimulus onset and decays after that. The high temporal resolution of EEG allowed us to detect how object space rapidly evolves over time, of which fMRI may not be sensitive to. We demonstrated that category and aspect ratio have distinct and differentiable temporal dynamics, both of which uniquely explain the neural data at different time points. Representations of these dimensions were modulated over time by binarizing the stimuli. Therefore, it is possible that the stimulus set confounding category and aspect ratio, combined with a lack of available category information (Bao et al., 2020), resulted in aspect ratio explaining category information in the macaque inferotemporal cortex data, while the available category information combined with the slower resolution of fMRI resulted in category information explaining the dimension of aspect ratio in human participants (Coggan & Tong, 2023; Yargholi & Op de Beeck, 2023). Overall, our results indicate that the dimensions of aspect ratio and category are both represented during object processing and one object space dimension does not fully explain the other dimension. Our data suggest that object space is flexible, and likely weights dimensions underlying object space differently depending on the visual information that is available.

Our results corroborate studies that have investigated the dissociation of visual features, such as aspect ratio and shape, from category information during object processing. While shape and aspect ratio are distinguishable from one another (Bougou et al., 2024; Bracci & Op de Beeck, 2016) and shape is an overall coarser and less standardized visual feature, they are highly related and will both be discussed here. In single-unit recordings in macaque inferotemporal cortex, visual features such as aspect ratio (along a gradient of round to thin shapes) better explained neural responses when compared with semantic or category information (Baldassi et al., 2013). Dissociations between category information and both aspect ratio and shape were also reported in human multi-unit activity and high-gamma responses in the Lateral Occipital Complex (Bougou et al., 2024). Similar findings have been reported when investigating shape. Within-body stimuli, shape information was preserved independent of category information, and this shape information was available earlier than category information (Kaiser, Azzalini, et al., 2016). Several fMRI (Bracci & Op de Beeck, 2016; Kriegeskorte et al., 2008; Op de Beeck et al., 2008; Proklova et al., 2016) and MEG (Carlson et al., 2013; Cichy et al., 2014, 2016; Contini et al., 2017) studies have also observed shape information independent of category information and vice versa during object processing. While

not all of these studies specifically dissociated category from shape within the presented stimuli, post hoc analysis accounting for visual properties found shape and category could not fully explain one another. Interestingly, for unfamiliar objects, the organization of human object-selective regions was strongly related to perceived shape information (Op de Beeck et al., 2008), supporting the idea that aspect ratio and shape information may be more strongly weighted when category and object identity information is not available. Our results extend this literature by exploring the temporal dynamics of object processing and stability of this information where category and aspect ratio are orthogonalized, and by masking internal object details in these same stimuli. Aspect ratio information is stronger and more stable over time in silhouette objects than in intact objects and is available earlier than category information in all objects. Moreover, aspect ratio information is generalizable over changes in other dimensions of object space, such as animacy. Future studies may benefit from explicitly investigating the relationship between object discernability and the temporal dynamics of object space dimensions, and by investigating whether this directly translates into performance on behavioral tasks that prioritize shape versus category (Grootswagers et al., 2018; Koenig-Robert et al., 2024).

While EEG is an ideal method to investigate rapidly occurring object information and characterize the temporal dynamics underlying object processing, it does not have the spatial resolution needed to investigate where this information originates in the cortex. A previous fMRI study did not observe strong representations of aspect ratio in object-selective regions, but instead found this information mainly originated in early visual areas, such as V1 (Yargholi & Op de Beeck, 2023). In our data, we observed a shift in the topography for animacy and category information in intact stimuli around 200 ms. While aspect ratio information primarily seemed to rely on occipital regions, animacy and category information suggested a shift to more occipito-temporal pattern. It is possible that the early and transient neural signals underlying aspect ratio information that we observed originate in early visual cortex, while category and animacy information originates in subsequent object-selective regions. Even though we cannot test this possibility directly, the spatial topography of the sensor searchlight analysis was largely preserved between aspect ratio, category, and animacy decoding during early processing and in the silhouette stimuli. These results may hint that signals underlying different object space dimensions originate in similar areas of the brain, but can flexibly engage different patterns of activity depending on the stimulus information available to the visual system. For example, intact stimuli with preserved internal details seem to rely more on lat-

eral regions to process animacy and category information when compared with aspect ratio information, whereas object stimuli with masked internal information may represent aspect ratio in similar regions as category and animacy. Our data may be capturing rapid and transient aspect ratio representations within object-selective cortex, and, therefore, converge with previous fMRI observations of weak aspect ratio information in regions such as rightFC-object and rLOC-object (Yargholi & Op de Beeck, 2023). To continue to investigate this possibility, it would be beneficial for future studies to use methods, such as MEG source space decoding and ECoG, that are sensitive to both spatial and temporal information. These methods would also provide a sensitive way to investigate the role of feedback during object processing, and how these feedback processes may differ between dimensions of object space. Previous studies have highlighted the importance of considering interactions of feedforward and feedback information during object processing (Bar, 2003; Gilbert & Li, 2013; Rao & Ballard, 1999). Using methods that are sensitive to spatiotemporal dynamics of object space could further elucidate how different dimensions of object space uniquely contribute to visual object processing. Finally, by leveraging these methods, the underlying dynamics of aspect ratio can be disentangled from other lower-level perceptual properties, such as pixel-level information. Our data demonstrate that pixel information uniquely explains neural variance from dimensions of object space, however, where this information originates in our data is unknown. It is also possible that, even though we were able to also decode category and animacy information, our EEG data could be biased toward low-level information (Proklova et al., 2019). Distinguishing pixel information, and other low-level visual properties, during object processing from aspect ratio and categorical-level object space dimensions in methods sensitive to both time and space can help to further understand how visual properties contribute to the visual object processing, and biases that may exist in other neuroimaging methods.

Recently, a new approach to investigating object processing has been proposed (Contier et al., 2024). When compared with traditional category or feature-driven approaches, object space dimensions (66 in total) derived from millions of behavioral responses could better explain neural responses across human visual cortex. These dimensions also replicated and explained previously reported feature and category selectivity (Contier et al., 2024). When investigating the temporal dynamics underlying these behaviorally relevant object space dimensions, multidimensional information was rapidly available (~80 ms) and physical object property information was available earlier than conceptual information (Teichmann

et al., 2023). These results highlight that object space is dynamic over time and that object processing needs to be considered more holistically than low-dimensional object spaces. Specifically, object processing is likely a result of a complex interplay between external stimulus information (Grootswagers, Robinson, & Carlson, 2019), co-occurring object dimensions (Guntupalli et al., 2016; Haxby et al., 2011) that are relevant for behavior (Contier et al., 2024; Grootswagers et al., 2018; Teichmann et al., 2023) or social interaction (Contini et al., 2020; Grootswagers et al., 2022), and are sensitive to task demands (Grootswagers et al., 2021; Kaiser, Oosterhof, et al., 2016) and individual differences (e.g. internal representations, cognitive abilities) (Bracci & Op de Beeck, 2023). Our results can be easily interpreted through this multidimensional framework, such that the object space dimensions we probed were distinct from one another even though they co-occurred, dynamically evolved over time, and were flexibly weighted depending on available stimulus information. In future studies, it would be helpful to investigate the temporal dynamics underlying behaviorally derived dimensions in both intact and silhouette stimuli across varying task demands to more fully characterize object processing and understand the importance of object space dimensions in different conditions over time.

In sum, the object space dimensions of aspect ratio, category, and animacy are all present and distinct from one another over time and differentially explain the representational structure of the neural data during object processing. The strength and stability of these dimensions are modulated by the availability of internal object details, suggesting that the object space is flexible and depends on the information available to the visual system. These results help resolve previously reported discrepancies in the literature and support a more multidimensional view of object space. Moreover, these data reinforce that temporal information is important to consider when investigating object processing. Object processing, and, therefore, object space, is not static and evolves over time, and should be investigated using methods that are sensitive to these dynamics.

DATA AND CODE AVAILABILITY

Code is available on GitHub (https://github.com/alexiskidder/ObjectProcessing_RSVP) and data are available on OpenNeuro (<https://openneuro.org/datasets/ds005648>).

AUTHOR CONTRIBUTIONS

Alexis Kidder: Conceptualization, Methodology, Software, Formal Analysis, Investigation, Data Curation,

Writing—Original Draft, Writing—Review & Editing, Visualization. Genevieve L. Quek: Conceptualization, Validation, Resources, Writing—Review & Editing, Supervision. Tijl Grootswagers: Conceptualization, Methodology, Software, Validation, Resources, Writing—Review & Editing, Supervision.

FUNDING

This work was supported by the International Visiting Scholar Program at The MARCS Institute for Brain, Behaviour, and Development, Western Sydney University and by the Australian Research Council grant DE230100380.

DECLARATION OF COMPETING INTEREST

The authors have declared that there are no conflicts of interest in relation to the subject of this study.

ACKNOWLEDGMENTS

The authors thank Lina Teichmann and Chris Baker for helpful discussions, and Mahdiyeh Khanbagi, Jessica Chin, Nazanin Sheykhan Andalibi, and Almudena Ramírez Haro for assistance with data acquisition and EEG methods.

REFERENCES

- Baldassi, C., Alemi-Neissi, A., Pagan, M., DiCarlo, J. J., Zecchina, R., & Zoccolan, D. (2013). Shape similarity, better than semantic membership, accounts for the structure of visual object representations in a population of monkey inferotemporal neurons. *PLoS Computational Biology*, 9(8), e1003167. <https://doi.org/10.1371/journal.pcbi.1003167>
- Bao, P., She, L., McGill, M., & Tsao, D. Y. (2020). A map of object space in primate inferotemporal cortex. *Nature*, 583(7814), 103–108. <https://doi.org/10.1038/s41586-020-2350-5>
- Bar, M. (2003). A cortical mechanism for triggering top-down facilitation in visual object recognition. *Journal of Cognitive Neuroscience*, 15(4), 600–609. <https://doi.org/10.1162/08989290321662976>
- Bougou, V., Vanhoyland, M., Bertrand, A., Van Paesschen, W., Op De Beeck, H., Janssen, P., & Theys, T. (2024). Neuronal tuning and population representations of shape and category in human visual cortex. *Nature Communications*, 15(1), 4608. <https://doi.org/10.1038/s41467-024-49078-3>
- Bracci, S., & Op De Beeck, H. (2016). Dissociations and associations between shape and category representations in the two visual pathways. *The Journal of Neuroscience*, 36(2), 432–444. <https://doi.org/10.1523/JNEUROSCI.2314-15.2016>
- Bracci, S., & Op De Beeck, H. P. (2023). Understanding human object vision: A picture is worth a thousand representations. *Annual Review of Psychology*, 74(1), 113–135. <https://doi.org/10.1146/annurev-psych-032720-041031>

- Carlson, T., Tovar, D. A., Alink, A., & Kriegeskorte, N. (2013). Representational dynamics of object vision: The first 1000 ms. *Journal of Vision*, 13(10), 1. <https://doi.org/10.1167/13.10.1>
- Carlson, T. A., Hogendoorn, H., Kanai, R., Mesik, J., & Turrey, J. (2011). High temporal resolution decoding of object position and category. *Journal of Vision*, 11(10), 9. <https://doi.org/10.1167/11.10.9>
- Carlson, T. A., Simmons, R. A., Kriegeskorte, N., & Slevc, L. R. (2014). The emergence of semantic meaning in the ventral temporal pathway. *Journal of Cognitive Neuroscience*, 26(1), 120–131. https://doi.org/10.1162/jocn_a_00458
- Chao, L. L., Haxby, J. V., & Martin, A. (1999). Attribute-based neural substrates in temporal cortex for perceiving and knowing about objects. *Nature Neuroscience*, 2(10), 913–919. <https://doi.org/10.1038/13217>
- Cichy, R. M., Pantazis, D., & Oliva, A. (2014). Resolving human object recognition in space and time. *Nature Neuroscience*, 17(3), 455–462. <https://doi.org/10.1038/nn.3635>
- Cichy, R. M., Pantazis, D., & Oliva, A. (2016). Similarity-based fusion of MEG and fMRI reveals spatio-temporal dynamics in human cortex during visual object recognition. *Cerebral Cortex*, 26(8), 3563–3579. <https://doi.org/10.1093/cercor/bhw135>
- Coggan, D. D., Liu, W., Baker, D. H., & Andrews, T. J. (2016). Category-selective patterns of neural response in the ventral visual pathway in the absence of categorical information. *NeuroImage*, 135, 107–114. <https://doi.org/10.1016/j.neuroimage.2016.04.060>
- Coggan, D. D., & Tong, F. (2023). Spikiness and animacy as potential organizing principles of human ventral visual cortex. *Cerebral Cortex*, 33(13), 8194–8217. <https://doi.org/10.1093/cercor/bhad108>
- Contier, O., Baker, C. I., & Hebart, M. N. (2024). Distributed representations of behaviour-derived object dimensions in the human visual system. *Nature Human Behaviour*, 8(11), 2179–2193. <https://doi.org/10.1038/s41562-024-01980-y>
- Contini, E. W., Goddard, E., Grootswagers, T., Williams, M., & Carlson, T. (2020). A humanness dimension to visual object coding in the brain. *NeuroImage*, 221, 117139. <https://doi.org/10.1016/j.neuroimage.2020.117139>
- Contini, E. W., Wardle, S. G., & Carlson, T. A. (2017). Decoding the time-course of object recognition in the human brain: From visual features to categorical decisions. *Neuropsychologia*, 105, 165–176. <https://doi.org/10.1016/j.neuropsychologia.2017.02.013>
- Gilbert, C. D., & Li, W. (2013). Top-down influences on visual processing. *Nature Reviews Neuroscience*, 14(5), 350–363. <https://doi.org/10.1038/nrn3476>
- Grootswagers, T., Cichy, R. M., & Carlson, T. A. (2018). Finding decodable information that can be read out in behaviour. *NeuroImage*, 179, 252–262. <https://doi.org/10.1016/j.neuroimage.2018.06.022>
- Grootswagers, T., McKay, H., & Varlet, M. (2022). Unique contributions of perceptual and conceptual humanness to object representations in the human brain. *NeuroImage*, 257, 119350. <https://doi.org/10.1016/j.neuroimage.2022.119350>
- Grootswagers, T., Robinson, A. K., & Carlson, T. A. (2019). The representational dynamics of visual objects in rapid serial visual processing streams. *NeuroImage*, 188, 668–679. <https://doi.org/10.1016/j.neuroimage.2018.12.046>
- Grootswagers, T., Robinson, A. K., Shatek, S. M., & Carlson, T. A. (2019). Untangling featural and conceptual object representations. *NeuroImage*, 202, 116083. <https://doi.org/10.1016/j.neuroimage.2019.116083>
- Grootswagers, T., Robinson, A. K., Shatek, S. M., & Carlson, T. A. (2021). The neural dynamics underlying prioritisation of task-relevant information. *Neurons, Behavior, Data Analysis, and Theory*, 5(1), 1–17. <https://doi.org/10.51628/001c.21174>
- Grootswagers, T., Quek, G., Zhen, Z., & Varlet, M. (2025). Human infant EEG recordings for 200 object images presented in rapid visual streams. *Scientific Data*, 12, 407. <https://doi.org/10.1038/s41597-025-04744-z>
- Grootswagers, T., Robinson, A. K., Shatek, S. M., & Carlson, T. A. (2024). Mapping the dynamics of visual feature coding: Insights into perception and integration. *PLoS Computational Biology*, 20(1), e1011760. <https://doi.org/10.1371/journal.pcbi.1011760>
- Grootswagers, T., Wardle, S. G., & Carlson, T. A. (2017). Decoding dynamic brain patterns from evoked responses: A tutorial on multivariate pattern analysis applied to time series neuroimaging data. *Journal of Cognitive Neuroscience*, 29(4), 677–697. https://doi.org/10.1162/jocn_a_01068
- Grootswagers, T., Zhou I., Robinson, A. K., Hebart, M. N., & Carlson, T. A. (2022). Human EEG recordings for 1,854 concepts presented in rapid serial visual presentation streams. *Scientific Data*, 9(1), 3. <https://doi.org/10.1038/s41597-021-01102-7>
- Guntupalli, J. S., Hanke, M., Halchenko, Y. O., Connolly, A. C., Ramadge, P. J., & Haxby, J. V. (2016). A model of representational spaces in human cortex. *Cerebral Cortex*, 26(6), 2919–2934. <https://doi.org/10.1093/cercor/bhw068>
- Haxby, J. V., Guntupalli, J. S., Connolly, A. C., Halchenko, Y. O., Conroy, B. R., Gobbini, M. I., Hanke, M., & Ramadge, P. J. (2011). A common, high-dimensional model of the representational space in human ventral temporal cortex. *Neuron*, 72(2), 404–416. <https://doi.org/10.1016/j.neuron.2011.08.026>
- Huang, T., Song, Y., & Liu, J. (2022). Real-world size of objects serves as an axis of object space. *Communications Biology*, 5(1), 749. <https://doi.org/10.1038/s42003-022-03711-3>
- Kaiser, D., Azzalini, D. C., & Peelen, M. V. (2016). Shape-independent object category responses revealed by MEG and fMRI decoding. *Journal of Neurophysiology*, 115(4), 2246–2250. <https://doi.org/10.1152/jn.01074.2015>
- Kaiser, D., Oosterhof, N. N., & Peelen, M. V. (2016). The neural dynamics of attentional selection in natural scenes. *The Journal of Neuroscience*, 36(41), 10522–10528. <https://doi.org/10.1523/JNEUROSCI.1385-16.2016>
- Kayaert, G., Biederman, I., Op De Beeck, H. P., & Vogels, R. (2005). Tuning for shape dimensions in macaque inferior temporal cortex. *European Journal of Neuroscience*, 22(1), 212–224. <https://doi.org/10.1111/j.1460-9568.2005.04202.x>
- King, J.-R., & Dehaene, S. (2014). Characterizing the dynamics of mental representations: The temporal generalization method. *Trends in Cognitive Sciences*, 18(4), 203–210. <https://doi.org/10.1016/j.tics.2014.01.002>
- Koenig-Robert, R., Quek, G. L., Grootswagers, T., & Varlet, M. (2024). Movement trajectories as a window into the dynamics of emerging neural representations. *Scientific Reports*, 14(1), 11499. <https://doi.org/10.1038/s41598-024-62135-7>
- Konkle, T., & Caramazza, A. (2013). Tripartite organization of the ventral stream by animacy and object size. *Journal of Neuroscience*, 33(25), 10235–10242. <https://doi.org/10.1523/JNEUROSCI.0983-13.2013>
- Konkle, T., & Oliva, A. (2012). A real-world size organization of object responses in occipitotemporal cortex. *Neuron*,

- 74(6), 1114–1124. <https://doi.org/10.1016/j.neuron.2012.04.036>
- Kriegeskorte, N., Mur, M., & Bandettini, P. A. (2008). Representational similarity analysis—Connecting the branches of systems neuroscience. *Frontiers in Systems Neuroscience*, 2. <https://www.frontiersin.org/journals/systems-neuroscience/articles/10.3389/neuro.06.004.2008>
- Kriegeskorte, N., Mur, M., Ruff, D. A., Kiani, R., Bodurka, J., Esteky, H., Tanaka, K., & Bandettini, P. A. (2008). Matching categorical object representations in inferior temporal cortex of man and monkey. *Neuron*, 60(6), 1126–1141. <https://doi.org/10.1016/j.neuron.2008.10.043>
- Morey, R. D., Rouder, J. N., Jamil, T., & Morey, M. D. R. (2015). Package “*BayesFactor*” [Computer software]. <https://cran.r-project.org/web/packages/BayesFactor/BayesFactor.pdf>
- Naselaris, T., Prenger, R. J., Kay, K. N., Oliver, M., & Gallant, J. L. (2009). Bayesian reconstruction of natural images from human brain activity. *Neuron*, 63(6), 902–915. <https://doi.org/10.1016/j.neuron.2009.09.006>
- Nasr, S., Echavarria, C. E., & Tootell, R. B. H. (2014). Thinking outside the box: Rectilinear shapes selectively activate scene-selective cortex. *The Journal of Neuroscience*, 34(20), 6721–6735. <https://doi.org/10.1523/JNEUROSCI.4802-13.2014>
- Oostenveld, R., Fries, P., Maris, E., & Schoffelen, J.-M. (2011). FieldTrip: Open source software for advanced analysis of MEG, EEG, and invasive electrophysiological data. *Computational Intelligence and Neuroscience*, 2011, 1–9. <https://doi.org/10.1155/2011/156869>
- Op De Beeck, H. P., Torfs, K., & Wagemans, J. (2008). Perceived shape similarity among unfamiliar objects and the organization of the human object vision pathway. *The Journal of Neuroscience*, 28(40), 10111–10123. <https://doi.org/10.1523/JNEUROSCI.2511-08.2008>
- Oosterhof, N. N., Connolly, A. C., & Haxby, J. V. (2016). CoSMoMVPA: Multi-modal multivariate pattern analysis of neuroimaging data in Matlab/GNU Octave. *Frontiers in Neuroinformatics*, 10. <https://doi.org/10.3389/fninf.2016.00027>
- O'Toole, A. J., Jiang, F., Abdi, H., & Haxby, J. V. (2005). Partially distributed representations of objects and faces in ventral temporal cortex. *Journal of Cognitive Neuroscience*, 17(4), 580–590. <https://doi.org/10.1162/0898929053467550>
- Peirce, J., Gray, J. R., Simpson, S., MacAskill, M., Höchenberger, R., Sogo, H., Kastman, E., & Lindeløv, J. K. (2019). PsychoPy2: Experiments in behavior made easy. *Behavior Research Methods*, 51(1), 195–203. <https://doi.org/10.3758/s13428-018-01193-y>
- Proklova, D., Kaiser, D., & Peelen, M. V. (2016). Disentangling representations of object shape and object category in human visual cortex: The animate–inanimate distinction. *Journal of Cognitive Neuroscience*, 28(5), 680–692. https://doi.org/10.1162/jocn_a_00924
- Proklova, D., Kaiser, D., & Peelen, M. V. (2019). MEG sensor patterns reflect perceptual but not categorical similarity of animate and inanimate objects. *NeuroImage*, 193, 167–177. <https://doi.org/10.1016/j.neuroimage.2019.03.028>
- Quek, G. L., Theodorou, A., & Peelen, M. V. (2025). The timecourse of inter-object contextual facilitation. *Cortex*, 190, 38–53. <https://doi.org/10.1016/j.cortex.2025.05.020>
- Rao, R., & Ballard, D. (1999). Predictive coding in the visual cortex: a functional interpretation of some extra-classical receptive-field effects. *Nature Neuroscience*, 2. <https://doi.org/10.1038/4580>
- Rice, G. E., Watson, D. M., Hartley, T., & Andrews, T. J. (2014). Low-level image properties of visual objects predict patterns of neural response across category-selective regions of the ventral visual pathway. *Journal of Neuroscience*, 34(26), 8837–8844. <https://doi.org/10.1523/JNEUROSCI.5265-13.2014>
- Robinson, A. K., Grootswagers, T., & Carlson, T. A. (2019). The influence of image masking on object representations during rapid serial visual presentation. *NeuroImage*, 197, 224–231. <https://doi.org/10.1016/j.neuroimage.2019.04.050>
- Robinson, A. K., Grootswagers, T., Shatek, S., Behrmann, M., & Carlson, T. A. (2025). Dynamics of visual object coding within and across the hemispheres: Objects in the periphery. *Science Advances*, 11(1), eadq0889. <https://doi.org/10.1126/sciadv.adq0889>
- Robinson, A. K., Quek, G. L., & Carlson, T. A. (2023). Visual representations: Insights from neural decoding. *Annual Review of Vision Science*, 9(1), 313–335. <https://doi.org/10.1146/annurev-vision-100120-025301>
- Rouder, J. N., Speckman, P. L., Sun, D., Morey, R. D., & Iverson, G. (2009). Bayesian t tests for accepting and rejecting the null hypothesis. *Psychonomic Bulletin & Review*, 16(2), 225–237. <https://doi.org/10.3758/PBR.16.2.225>
- Sha, L., Haxby, J. V., Abdi, H., Guntupalli, J. S., Oosterhof, N. N., Halchenko, Y. O., & Connolly, A. C. (2015). The animacy continuum in the human ventral vision pathway. *Journal of Cognitive Neuroscience*, 27(4), 665–678. https://doi.org/10.1162/jocn_a_00733
- Shatek, S. M., Robinson, A. K., Grootswagers, T., & Carlson, T. A. (2022). Capacity for movement is an organisational principle in object representations. *NeuroImage*, 261, 119517. <https://doi.org/10.1016/j.neuroimage.2022.119517>
- Teichmann, L., Moerel, D., Baker, C., & Grootswagers, T. (2022). An empirically driven guide on using Bayes factors for M/EEG decoding. *Aperture Neuro*, 2, 1–10. <https://doi.org/10.52294/ApertureNeuro.2022.2.MAOC6465>
- Teichmann, L., Hebart, M. N., & Baker, C. I. (2023). Dynamic representation of multidimensional object properties in the human brain. *bioRxiv* [Preprint]. <https://doi.org/10.1101/2023.09.08.556679>
- Thorat, S., Proklova, D., & Peelen, M. V. (2019). The nature of the animacy organization in human ventral temporal cortex. *eLife*, 8, e47142. <https://doi.org/10.7554/eLife.47142>
- Yargholi, E., & Op De Beeck, H. (2023). Category trumps shape as an organizational principle of object space in the human occipitotemporal cortex. *The Journal of Neuroscience*, 43(16), 2960–2972. <https://doi.org/10.1523/JNEUROSCI.2179-22.2023>